An assessment of two models for the subgrid scale tensor in the rational LES model

Volker John*

Institut für Analysis und Numerik, Fakultät für Mathematik Otto-von-Guericke-Universität Magdeburg, Postfach 4120, Magdeburg D-39016, Germany

Abstract

LES models seek to approximate the large scales of a flow which are defined by a space average $(\bar{\mathbf{u}}, \bar{p})$ of the velocity $\mathbf{u}$ and the pressure p of the flow. A natural question which arises is: Given reliable data for $(\bar{\mathbf{u}}, \bar{p})$, how accurate is the approximation of $(\bar{\mathbf{u}}, \bar{p})$ by the solution computed with a LES model? This paper presents numerical studies of this question at a 2d and 3d mixing layer problem for the rational LES model with two types of models for the subgrid scale tensor: the Smagorinsky model and a model proposed by Iliescu and Layton. Whereas in the 2d mixing layer problem the model by Iliescu and Layton showed better results, the behaviour of both models was similar in the 3d mixing layer problem.

1. Introduction

Incompressible flows are governed by the incompressible Navier–Stokes equations

$$\mathbf{u}_t - 2\nu\nabla \cdot \mathbb{D}(\mathbf{u}) + (\mathbf{u} \cdot \nabla)\mathbf{u} + \nabla p = \mathbf{f} \quad \text{in } (0, T] \times \Omega,$$

$$\nabla \cdot \mathbf{u} = 0 \quad \text{in } (0, T] \times \Omega,$$

$$\mathbf{u}(0, \cdot) = \mathbf{u}_0 \quad \text{in } \Omega. \tag{1}$$

* Tel.: +49-391-67-12633; fax: +49-391-67-18073.
 E-mail address: john@mathematik.uni-magdeburg.de (V. John).
 URL: http://www-ian.math.uni-magdeburg.de/home/john/

Here, $\mathbf{u}$ is the velocity, $\mathbb{D}(\mathbf{u}) = (\mathbf{u} + \mathbf{u}^T)/2$ the velocity deformation tensor, p the pressure, $\mathbf{f}$ represents body forces, v is the kinematic viscosity, $\Omega \subset \mathbb{R}^d$, $d = 2, 3$ is a domain and T the end of a time interval. If Ω is a bounded domain, (1) has to be equipped with boundary conditions.

This paper considers a model which has been developed for the large eddy simulation (LES) of turbulent flows. Turbulent flows are characterised by a small viscosity v or a large Reynolds number $Re = \mathcal{O}(v^{-1})$. A direct numerical simulation (DNS) of (1) would seek to resolve all persisting scales of the flow. This is in general, in particular in 3d, not possible. Turbulence models are necessary to obtain equations which, on the one hand, can be treated numerically and, on the other hand, whose solution should preserve important properties of the solution of (1). LES is currently a popular and promising approach of modelling turbulence, see [28,15] for overviews of the state of art from the engineering and the mathematical point of view, respectively.

LES seeks to compute accurately all scales larger or equal than a prescribed size. To this end, the velocity and the pressure are decomposed into

$$\mathbf{u} = \bar{\mathbf{u}} + \mathbf{u}', \quad p = \bar{p} + p', \tag{2}$$

where $(\bar{\mathbf{u}}, \bar{p})$ are the large scale flow structures and the remainder $(\mathbf{u}', p')$ represents the small flow structures. The large scale flow structures are defined by averaging $(\mathbf{u}, p)$ in space. Let $\Omega = \mathbb{R}^d$ for the moment. In this paper, the averaging is defined by convolution with the Gaussian filter

$$g_\delta(\mathbf{x}) = \left(\frac{6}{\delta^2 \pi} \right)^{d/2} \exp \left(-\frac{6}{\delta^2} \|\mathbf{x}\|_2^2 \right), \tag{3}$$

where $\delta > 0$ is the filter width and $\|\mathbf{x}\|_2$ the Euclidean norm of $\mathbf{x} \in \mathbb{R}^d$. Thus $\bar{\mathbf{u}} = g_\delta * \mathbf{u}$, $\bar{p} = g_\delta * p$ represent the flow structures of size $\mathcal{O}(\delta)$. The filter function filters out the small scales or, equivalently, damps the high wave number components of the flow.

The first step to obtain equations for $(\bar{\mathbf{u}}, \bar{p})$ consists in filtering the Navier–Stokes equations (1). One obtains the space averaged Navier–Stokes equations

$$\bar{\mathbf{u}}_t - 2v \nabla \cdot \mathbb{D}(\bar{\mathbf{u}}) + \nabla \cdot (\overline{\mathbf{u} \mathbf{u}^T}) + \nabla \bar{p} = \bar{\mathbf{f}} \quad \text{in } (0, T] \times \mathbb{R}^d,$$

$$\nabla \cdot \bar{\mathbf{u}} = 0 \quad \text{in } [0, T] \times \mathbb{R}^d,$$

$$\bar{\mathbf{u}}(0, \cdot) = \bar{\mathbf{u}}_0 \quad \text{in } \mathbb{R}^d, \tag{4}$$

where the Reynolds stress tensor can be decomposed into

$$\overline{\mathbf{u} \mathbf{u}^T} = \overline{\bar{\mathbf{u}} \bar{\mathbf{u}}^T} + \overline{\bar{\mathbf{u}} \mathbf{u}'^T} + \overline{\mathbf{u}' \bar{\mathbf{u}}^T} + \overline{\mathbf{u}' \mathbf{u}'^T} \tag{5}$$

by applying (2). The entries of the Reynolds stress tensor are á priori not related to $(\bar{\mathbf{u}}, \bar{p})$. It arises a closure problem since there are more unknowns than equations in (4). A main issue in LES is to model the Reynolds stress tensor in terms of $(\bar{\mathbf{u}}, \bar{p})$.

Many models of the Reynolds stress tensor can be found in the literature. One of the most simple and popular ones is the Smagorinsky model [29], which will be considered in this paper as model for the subgrid scale tensor $\overline{\mathbf{u}' \mathbf{u}'^T}$ within the rational LES model. The Smagorinsky model, like other LES models, is based on physical considerations. But there have been also attempts to obtain LES models by mathematical derivations. Well-known is the gradient model (sometimes called Taylor LES model) which goes back to [21] and was improved in [2]. The main ideas of deriving this
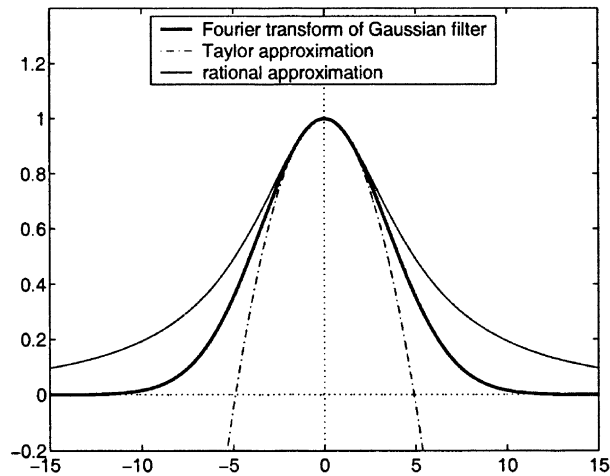
Fig. 1. The Fourier transform of the Gaussian filter with its Taylor polynomial approximation (7) and its rational approximation (8).

model will be sketched in Section 2. The key in its derivation is the approximation of the Fourier transform of the Gaussian filter by a simpler function. In [21,2], an approximation by a second order Taylor polynomial is proposed. A study of this approximation reveals, however, that the damping of the high wave number components of the flow cannot be expected by the Taylor polynomial. Whereas the Fourier transform of the Gaussian filter is almost zero for the high wave numbers, the Taylor polynomial tends to $-\infty$, see Fig. 1. Based on this observation, in [7] was proposed to use a second order rational approximation of the Fourier transform of the Gaussian filter which tends to zero for high wave numbers. The resulting LES model will be called rational LES model and its derivation is reviewed in Section 2.

The subgrid scale term $\overline{\mathbf{u}'\mathbf{u}'^{T}}$ of the right-hand side of (5) will be modelled by $\mathbf{0}$ in the rational LES model. This has been proven to be insufficient in numerical tests [12,15]. The main goal of this paper is an assessment of two alternative models for $\overline{\mathbf{u}'\mathbf{u}'^{T}}$ which have been proposed in the literature: the Smagorinsky model and the Iliescu–Layton model proposed in [13].

The main purpose of LES models is to provide an accurate approximation of $(\overline{\mathbf{u}}, \bar{p})$. A natural and very important question is: *How good is the approximation of $(\overline{\mathbf{u}}, \bar{p})$ by the flow field computed with LES models*? Since the derivation of the rational LES model is valid in two and three dimensions, for arbitrary Reynolds numbers *Re* and for arbitrary filter widths δ, the study of this question is of interest from the point of view of the theory of the rational LES model for all these situations. The performance of numerical tests studying this question requires reliable data for $(\overline{\mathbf{u}}, \bar{p})$ in time and space. Such data are not available for the most interesting situation, which is 3d turbulent flow. But only if there is a positive answer of this question for a LES model in situations which are manageable, there is a well founded hope that this model yields good results also in situations like 3d turbulent flow.

The paper studies the above formulated question for the rational LES model with the two models of the subgrid scale tensor $\overline{\mathbf{u}'\mathbf{u}'^{T}}$ in two situations where reliable data for $(\overline{\mathbf{u}}, \bar{p})$ can be computed,

namely a 2d mixing layer problem at higher Reynolds number $Re = 10\,000$ and a 3d mixing layer problem at lower Reynolds number $Re = 200$. To this end, a numerical study including the following steps:

1. approximate $(\mathbf{u}, p)$ by a DNS on a fine grid, denote the result by $(\mathbf{u}^h, p^h)$,
2. filter $(\mathbf{u}^h, p^h)$ which gives $(\overline{\mathbf{u}^h}, \overline{p^h})$,
3. solve the equations on a coarser grid with the rational LES model and the different models of the subgrid scale term and compare them to $(\overline{\mathbf{u}^h}, \overline{p^h})$,

was performed.

   The plan of the paper is as follows. The derivation of the rational LES model is reviewed in Section 2. Section 3 presents the numerical methods which are used in the solution of the LES model equations. The numerical study of the 2d mixing layer problem is presented in Section 4 and the numerical study of the 3d mixing layer problem in Section 5. Section 6 contains a summary of the results obtained in these studies.

2. The rational LES model

   The rational LES model is mainly based on mathematical derivations and not on physical considerations. The idea of deriving LES models in a mathematical way goes back to [21]. The first step consists in transforming (5) to the wave number space by a Fourier transform. This gives

$$\mathscr{F}(\overline{\mathbf{u}\mathbf{u}^T}) = \mathscr{F}(g_\delta)(\mathscr{F}(\overline{\mathbf{u}}\,\overline{\mathbf{u}}^T) + \mathscr{F}(\overline{\mathbf{u}}) * \mathscr{F}(\mathbf{u}')^T + \mathscr{F}(\mathbf{u}') * \mathscr{F}(\overline{\mathbf{u}})^T + \mathscr{F}(\mathbf{u}') * \mathscr{F}(\mathbf{u}')^T). \tag{6}$$

Since one likes to model (5) in terms of $\overline{\mathbf{u}}$, one has to replace $\mathbf{u}'$. From (2) and $\mathscr{F}(g_\delta) \neq 0$ follow

$$\mathscr{F}(\mathbf{u}') = \mathscr{F}(\mathbf{u}) - \mathscr{F}(\overline{\mathbf{u}}) = \frac{\mathscr{F}(g_\delta)\mathscr{F}(\mathbf{u})}{\mathscr{F}(g_\delta)} - \mathscr{F}(\overline{\mathbf{u}}) = \left(\frac{1}{\mathscr{F}(g_\delta)} - 1 \right) \mathscr{F}(\overline{\mathbf{u}}).$$

This is inserted into (6).

   The essential step in the derivation of the LES model consists now in replacing $\mathscr{F}(g_\delta)$ by a simpler function. The approach of Leonard [21], which was improved in [2], uses a second order Taylor polynomial approximation

$$\mathscr{F}(g_\delta)(\delta, \mathbf{y}) = 1 - \frac{\|\mathbf{y}\|_2^2}{24} \delta^2 + \mathcal{O}(\delta^4), \tag{7}$$

see also Fig. 1. The arising LES model has several names in the literature, e.g. gradient model or Taylor LES model. The essential property of the filter function, to filter out the small scales, is reflected in wave number space by very small absolute values of the Fourier transform of the filter function for high wave numbers, e.g. $\mathscr{F}(g_\delta)$ is very small for $\|\mathbf{y}\|_2$ large, see Fig. 1. It can be seen in Fig. 1 that the Taylor polynomial approximation of $\mathscr{F}(g_\delta)$ does not posses this property. In contrast, this approximation has very large negative values for $\|\mathbf{y}\|_2$ large. Thus, it can be expected that the (unmodified) Taylor LES model will rather intensify small flow structures than filter them out. This expectation has been supported by numerical studies [12,15], where solutions computed with the Taylor LES model blew up very fast. Therefore, this model is used in general with appropriate modifications which prevent blow-ups.

In [7], it is proposed to use a second order rational approximation of the exponential

$$e^{ax} = \frac{1}{1 + ax} + \mathcal{O}(a^2 x^2).$$

Applying this subdiagonal Padé approximation to $\mathscr{F}(g_\delta)$ gives

$$\mathscr{F}(g_\delta)(\delta, \mathbf{y}) = \frac{1}{1 + \|\mathbf{y}\|_2^2 \delta^2/24} + \mathcal{O}(\delta^4). \tag{8}$$

It can be observed, Fig. 1, that this approximation tends to zero for $\|\mathbf{y}\|_2 \to \infty$. Thus, the behaviour of $\mathscr{F}(g_\delta)$ for $\|\mathbf{y}\|_2 \to \infty$ is approximated correctly by the rational approximation. Inserting (8) into (6), neglecting all terms which are formally of fourth order in δ and applying the inverse Fourier transform give the rational LES model for the Reynolds stress tensor

$$\overline{\mathbf{u}}\,\overline{\mathbf{u}}^T + \overline{\overline{\mathbf{u}}\,\mathbf{u}'^T} + \overline{\mathbf{u}'\overline{\mathbf{u}}^T} \approx \left(I - \frac{\delta^2}{24}\Delta\right)^{-1} \left[\overline{\mathbf{u}}\,\overline{\mathbf{u}}^T - \frac{\delta^2}{24}(\overline{\mathbf{u}}\Delta(\overline{\mathbf{u}})^T + \Delta(\overline{\mathbf{u}})\overline{\mathbf{u}}^T)\right],$$

$$= \overline{\mathbf{u}}\,\overline{\mathbf{u}}^T + \frac{\delta^2}{12}\left(I - \frac{\delta^2}{24}\Delta\right)^{-1} \nabla\overline{\mathbf{u}}\nabla\overline{\mathbf{u}}^T, \tag{9}$$

$$\overline{\mathbf{u}'\mathbf{u}'^T} \approx \mathbf{0}. \tag{10}$$

The operator $(I - (\delta^2/24)\Delta)^{-1}$ describes an elliptic, second order problem which has to be solved. This problem will be called auxiliary problem. The auxiliary problem is an approximation of the convolution operator. From (8) follows

$$\mathscr{F}(g_\delta * \mathbf{u}) = \mathscr{F}(g_\delta)\mathscr{F}(\mathbf{u}) \approx \frac{1}{1 + \|\mathbf{y}\|_2^2 \delta^2/24}\mathscr{F}(\mathbf{u}) = \mathscr{F}\left(\left(I - \frac{\delta^2}{24}\Delta\right)^{-1}\mathbf{u}\right),$$

such that

$$g_\delta * \mathbf{u} \approx \left(I - \frac{\delta^2}{24}\Delta\right)^{-1}\mathbf{u}. \tag{11}$$

The so-called subgrid scale term $\overline{\mathbf{u}'\mathbf{u}'^T}$ is considered to be important for the development of turbulence. It is simply neglected by approximating it by $\mathbf{0}$ as in (10). Numerical studies in [12,15] show that solutions computed with the rational LES model and without model for the subgrid scale term generally blow up in finite time. Thus, there is the need of a model for this term. We will study two models which are proposed in the literature. The first one is the Smagorinsky model [29],

$$\overline{\mathbf{u}'\mathbf{u}'^T} \approx c_S \delta^2 \|\mathbb{D}(\overline{\mathbf{u}})\|_F \mathbb{D}(\overline{\mathbf{u}}). \tag{12}$$

This model was used in [3] as subgrid scale term in the Taylor LES model. The Smagorinsky model by itself is a simple and popular LES model. Many of its drawbacks are known, e.g. see [32]. But because of its simplicity, it is still widely used. In addition, a lot of mathematical support is available for the Smagorinsky model, e.g. existence and uniqueness of weak solutions [19], and finite element error analysis [16]. The second model for the subgrid scale term has been proposed by Iliescu and

Layton in [13]

$$\overline{\mathbf{u}'\mathbf{u}'^T} \approx c_\mathrm{S}\delta\|\overline{\mathbf{u}} - g_\delta * \overline{\mathbf{u}}\|_2 \mathbb{D}(\overline{\mathbf{u}}). \tag{13}$$

The convolution operator in (13) is approximated by (11) in the computations such that we use

$$\overline{\mathbf{u}'\mathbf{u}'^T} \approx c_\mathrm{S}\delta \left\| \overline{\mathbf{u}} - \left(I - \frac{\delta^2}{24}\Delta \right)^{-1} \overline{\mathbf{u}} \right\|_2 \mathbb{D}(\overline{\mathbf{u}}). \tag{14}$$

Both models for the subgrid scale term, the Smagorinsky model and the Iliescu–Layton model are based on physical arguments, see [29,13] for details.

To have a clear distinction between the large scale quantities $(\overline{\mathbf{u}}, \bar{p})$ and their approximations, we will denote the solution obtained by the LES models by $(\mathbf{w}, r)$.

The derivation of the space averaged Navier–Stokes equations (4) and the rational LES model (9) was done in $\mathbb{R}^d$. However, flow problems have to be computed in general in bounded domains $\Omega \subset \mathbb{R}^d$. The common way is simply to restrict the averaged Navier–Stokes equations and the rational LES model from $\mathbb{R}^d$ to Ω. This gives the LES model

$$\mathbf{w}_t - \nabla \cdot ((2\nu + \nu_\mathrm{T})\mathbb{D}(\mathbf{w})) + (\mathbf{w} \cdot \nabla)\mathbf{w} + \nabla r + \nabla \cdot \frac{\delta^2}{12}(A(\nabla\mathbf{w}\nabla\mathbf{w}^T)) = \overline{\mathbf{f}} \quad \text{in } (0, T] \times \Omega,$$

$$\nabla \cdot \mathbf{w} = 0 \quad \text{in } [0, T] \times \Omega,$$

$$\mathbf{w}(0, \cdot) = \mathbf{w}_0 \quad \text{in } \Omega,$$

$$+\text{boundary conditions.} \tag{15}$$

The operator A depends on the approximation of the Fourier transform of the Gaussian filter and the turbulent viscosity ν_T on the model for the subgrid scale term. In this paper, we consider the following models:

1. rational LES model with Smagorinsky subgrid scale model: $A = (I - (\delta^2/24)\Delta)^{-1}$ and ν_T given in (12),
2. rational LES model with Iliescu–Layton subgrid scale model: $A = (I - (\delta^2/24)\Delta)^{-1}$ and ν_T given in (14).

The Smagorinsky model is obtained by choosing $A = 0$ and ν_T as given in (12) and the Taylor LES model is obtained by choosing A as the identity.

The simple restriction of the equations from $\mathbb{R}^d$ to Ω leads of course to an error. This error will be particularly large near the boundary $\partial\Omega$ of Ω. An error which occurs by restricting the space average Navier–Stokes equations to a bounded domain, a so-called commutation error, has been analysed in [5]. It turned out that the commutation error does not necessarily vanish as the filter width δ tends to zero. An analysis of the restriction error of the rational LES model is not yet available.

From the restriction of the LES models to a bounded domain arises also the necessity of boundary conditions for (15) and also for the auxiliary problem in the rational LES model. Appropriate boundary conditions for the large eddies are an active field of research and many questions are still open. The most common way is to modify the LES model near a boundary to obtain reasonable solutions. However, such modifications may dominate principal properties of a LES model. Therefore,

we will consider flows whose turbulent regions are away from boundaries of the domain such that the choice of correct boundary conditions is not of vital importance. For the auxiliary problem in the rational LES model, we use homogeneous Neumann boundary conditions as proposed in [7]. On periodic boundaries, the auxiliary problem is equipped with periodic boundary conditions, too.

3. The numerical methods for solving (15)

The numerical tests were performed with the code MooNMD [18].

Problem (15) is first discretised in time by the fractional-step θ-scheme. This is an implicit second order scheme which is a popular discretisation for solving time-dependent Navier–Stokes equations, see [30].

There are three nonlinear terms in (15). Let $\mathbf{w}_k$ be the velocity at the discrete time t_k and $\mathbf{w}_{k-1}$ at the previous discrete time t_{k-1}. The nonlinear term coming from the rational LES model is treated explicitly, i.e.

$$\left(I - \frac{\delta^2}{4\gamma}\Delta\right)^{-1}(\nabla\mathbf{w}_k\nabla\mathbf{w}_k^T) \approx \left(I - \frac{\delta^2}{4\gamma}\Delta\right)^{-1}(\nabla\mathbf{w}_{k-1}\nabla\mathbf{w}_{k-1}^T) \tag{16}$$

and a semi-implicit form of the Iliescu–Layton model (14)

$$c_S\delta\left\|\mathbf{w}_k - \left(I - \frac{\delta^2}{4\gamma}\Delta\right)^{-1}\mathbf{w}_{k-1}\right\|_2 \mathbb{D}(\mathbf{w}_k) \tag{17}$$

is used. Thus, we have to solve the auxiliary problem in (16) and (17) only once in each discrete time where the velocity of the previous time is used to define the right-hand sides. All other terms are treated implicitly in time, in particular the convective term.

The arising system in time t_k is transformed into a variational formulation. One obtains an nonlinear saddle point problem to solve. The nonlinear problem is linearised by a fixed point iteration and the arising linear saddle point problems are discretised by an inf–sup stable finite element method, for details see [15]. The computations in 2d were carried out on quadrilateral grids and in 3d on hexahedral grids. The Q_2/P_1^{disc} pair of finite elements was used, i.e. the velocity is approximated by continuous piecewise biquadratics (2d) or triquadratics (3d) and the pressure by discontinuous linears. This is a very popular pair of finite element spaces in computational fluid dynamics, see [6,10], and it has been proven to combine a good accuracy and an efficient solvability of the linear saddle point problems by multilevel methods [14,17].

The auxiliary problems are discretised by a finite element method with Q_2 elements. They are solved iteratively with a preconditioned conjugate gradient (PCG) method with a SSOR preconditioner. Since the changes in the right-hand side for the auxiliary problems from time t_{k-1} to t_k are in general small, the solution of time t_{k-1} provides a good initial guess in the iteration for time t_k. Thus, in general, only few PCG iterations were necessary to solve the auxiliary problems. Altogether, the computational costs for solving the auxiliary problems were negligible in comparison to solving the nonlinear saddle point problems.

4. A mixing layer problem in two dimensions

This section presents a numerical study of a 2d mixing layer problem at $Re = 10\,000$. Numerical studies with this problem, also including LES models, can be found, e.g. in [1,11,23,26].

4.1. The definition of the problem and the set-up of the numerical tests

4.1.1. The definition of the problem

The problem is defined in $\Omega = (-1,1)^2$. Free-slip boundary conditions are applied at $y = -1$ and $y = 1$. At $x = 1$ and $x = -1$, periodic boundary conditions are prescribed. The initial velocity is given by

$$\mathbf{w}_0 = \begin{pmatrix} W_\infty \tanh\left(\dfrac{2y}{\sigma_0}\right) \\ 0 \end{pmatrix} + c_{\text{noise}} W_\infty \begin{pmatrix} \dfrac{\partial \psi}{\partial y} \\ -\dfrac{\partial \psi}{\partial x} \end{pmatrix} \tag{18}$$

with

$$\psi = \exp(-(2y/\sigma_0)^2)(\cos(8\pi x) + \cos(20\pi x)).$$

An illustration of the first component of the initial velocity field is presented in Fig. 2. There are no body forces in this mixing layer problem such that $\bar{\mathbf{f}} = \mathbf{0}$ in (15).

The mixing layer problem in two dimensions is well analysed, e.g. see [22, Section 3.3.1]. The problem is known to be inviscidly unstable. Slight perturbations in the initial condition are amplified by the so-called Kelvin–Helmholtz instabilities. The most amplified mode corresponds to the wave length $\lambda_a = 7\sigma_0$, see [25]. For a domain having the extension l_x in x direction with $l_x = n\lambda_a$, $n \in \mathbb{N}$, the number of primary vortices which are expected to develop is equal to n, see [22, p. 312].

We will present computations with four primary vortices, i.e. $n = 4$. Since $l_x = 2$, it follows that we have to choose $\sigma_0 = \frac{1}{14}$. The other parameters in the computations are chosen to be $W_\infty = 1$, scaling factor $c_{\text{noise}} = 0.001$ and viscosity $v^{-1} = 140\,000$. The Reynolds number of this flow, based on σ_0, W_∞ and v is $Re = (\sigma_0 W_\infty)/v = 10\,000$.
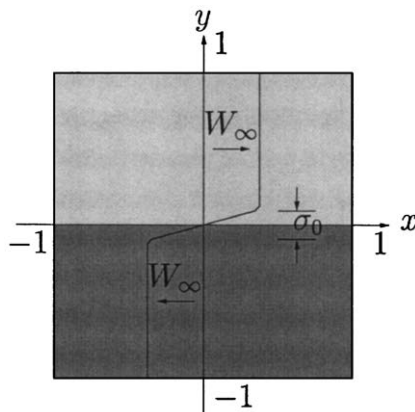

Fig. 2. First component of the initial velocity for the mixing layer problem in 2d (without noise).

Table 1
Degrees of freedom and mesh width on different levels

Level	h	Velocity	Pressure	Total
5	$\sqrt{2}/32$	33 024	12 288	45 312
8	$\sqrt{2}/256$	2 099 200	786 432	2 885 632

4.1.2. The vorticity thickness and the total kinetic energy

For the evaluation of the computational results, we consider the vorticity ω of the flow. The vorticity is the curl of the velocity $\mathbf{w} = (w_1, w_2)^T$ which is given by $\omega = (w_2)_x - (w_1)_y$. The vorticity thickness $\sigma(t)$ is defined by

$$\sigma(t) = \frac{2W_\infty}{\sup_{y \in [-1,1]} |\langle \omega \rangle (t, y)|}, \tag{19}$$

where $\langle \omega \rangle (t, y)$ is the integral mean in periodic direction

$$\langle \omega \rangle (t, y) = \frac{\int_{-1}^1 \omega(t, x, y)\, dx}{\int_{-1}^1 dx} = \frac{1}{2} \int_{-1}^1 \omega(t, x, y)\, dx.$$

In the computations, the term $2W_\infty / |\langle \omega \rangle (t, y)|$ can be computed only for a finite number of values y. We compute this term on all grid lines which are parallel to the x-axis. From the values computed in this way, the maximum is taken to obtain $\sigma(t)$. In the evaluation of the computations, we consider the vorticity thickness relative to σ_0: $\sigma(t)/\sigma_0$.

Besides the relative vorticity thickness, we study also the total kinetic energy of the computed solutions $\mathbf{w}^h$ given by

$$E_{\text{kin}}^h(t) = \frac{1}{2} \int_\Omega \mathbf{w}^h(t, \mathbf{x}) \cdot \mathbf{w}^h(t, \mathbf{x})\, d\mathbf{x}.$$

4.1.3. The discretisation in time and space, parameters of the LES models

A time unit $\bar{t} = \sigma_0 / W_\infty$ is defined and an equal distant time step of length $\Delta t_n = 0.1\bar{t} = 0.1/14 \approx 7.1428e - 3$ is used. The final time is set to be $T = 200\bar{t} \approx 14.285$.

The initial computational grid (level 0), consists of four squares of edge length one. This grid is refined uniformly and the number of degrees of freedom on finer levels is presented in Table 1. The filter width δ was chosen in all tests to be $\delta = h$, where h denotes as usual the diameter of the mesh cells, see Table 1. This choice makes sense for the second order velocity finite element space since each averaging circle with a degree of freedom as centre and with radius δ contains several neighbour degrees of freedom, see Fig. 3.

4.1.4. Evolution of the flow

The evolution of the flow can be described with the help of Fig. 4.[1] These pictures are the result of a DNS (Galerkin discretisation of the Navier–Stokes equations) on level 8. They present the

---

[1] The vorticity isolines in this section were plotted using the software package GRAPE.
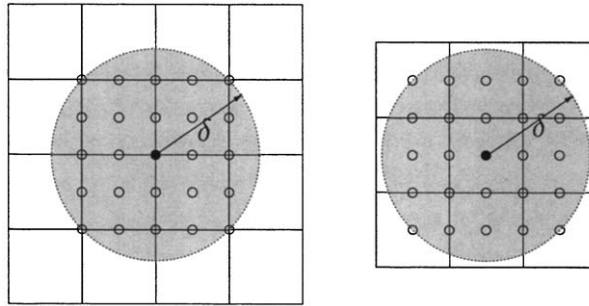
Fig. 3. Averaging circle for second order velocity with a degree of freedom as centre and radius $\delta = h$.
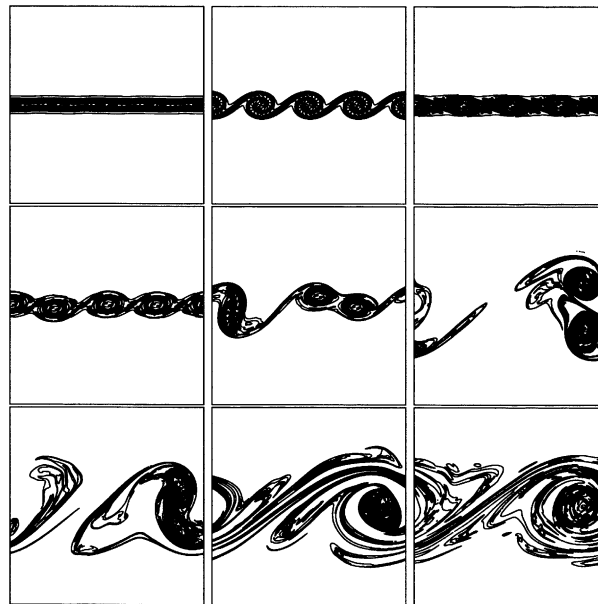

Fig. 4. Vorticity of $\overline{\mathbf{u}^h}$, level 8, at time units 20, 30, 50, 70, 80, 100, 120, 140, 200 (left to right, top to bottom).

evolution of the vorticity of $\overline{\mathbf{u}^h}$, where the filter width was chosen to be $\delta = \sqrt{2}/32$. This is the same filter width which was used for the computations with the LES models. The vorticity isolines are drawn for $\omega = 1 + 2k$ with $k \in \mathbb{Z}$ in all pictures. The evolution of the relative vorticity thickness resulting from $\overline{\mathbf{u}}^h$ is presented, e.g. in Fig. 10.

- *Development of the four primary eddies.* Starting with the initial noise, the four primary vortices develop. They can be seen clearly after 30 time units. The vorticity thickness is approximately doubled in comparison to the initial vorticity thickness σ_0.
- *Pairing of the four primary eddies.* It can be seen that one of these pairings starts earlier than the other one. At time unit 80, the different developments of both pairings are obviously. The

resulting eddies are called secondary eddies. The pairing of the four primary eddies is connected with another doubling of the relative vorticity thickness whose value is around 4 at time unit 80.
- *Pairing of the two secondary eddies.* The pairing of the four primary eddies into pairs of two is succeeded immediately by the pairing of these two secondary eddies into one eddy, see time unit 100. The relative vorticity thickness reaches values of more than 6. The pairing is in principal finished at time unit 140.
- *Rotation of the final eddy.* After time unit 140, the final eddy rotates at a rather fixed position. Since this eddy has an elliptic shape, the relative vorticity thickness oscillates and it takes values between 4 and 6.

The rational LES model was applied on level 5. The Galerkin discretisation of the Navier–Stokes equations blows up on this level after approximately 20 time units. Also the rational LES model without subgrid scale term blows up already in forming the four primary eddies, between time unit 12 and 13. This shows the necessity of using a model for the subgrid scale term.

4.2. The rational LES model with Smagorinsky subgrid scale term

The rational LES model with Smagorinsky subgrid scale term was applied with the scaling factors $c_S = 0.01$ and 0.005. The first value is typical for the Smagorinsky model if this model is used as LES model. If only the subgrid scale tensor is modelled with this model, it is reasonable to weaken its influence by using also smaller values for c_S.

4.2.1. The scaling factor $c_S = 0.01$
The evolution of the vorticity is presented in Fig. 5.
The main characteristics of the computed flow are as follows:

- *Development of the four primary eddies.* The development of the four primary eddies is computed very badly. In the reference solution, Fig. 4, these eddies are clearly seen at time unit 30 whereas these eddies can hardly be recognised in Fig. 5. There is also a clear difference in the development of the relative vorticity thickness, Fig. 10. For the reference solution, one can observe a rapid increase from 1 to 2 between time unit 25 and 30 while for the considered LES model, the increase from 1 to 2 is very slowly and it takes place from time unit 10 to 80. The four primary eddies are very flat in comparison to the reference solution. After time unit 50, they seem to disappear again.
- *Pairing of the four primary eddies.* This pairing starts after time unit 80 and it is connected with an increase of the relative vorticity thickness from 2 to 4. The beginning of the pairing is too late. This pairing is finished at time unit 100. A nonsimultaneous pairing cannot be observed.
- *Pairing of the two secondary eddies.* This pairing occurs immediately after the previous pairing. This is like in the reference solution. Since the pairing of the four primary eddies happened too late, also the pairing of the two secondary eddies takes place too late, at around time unit 130. The relative vorticity thickness reaches values of around 12.
- *Rotation of the final eddy.* The final eddy rotates with a somewhat lower speed than the final eddy of the reference solution. This can be seen at the lower frequency of the oscillation of the relative vorticity thickness in Fig. 10. The values of the relative vorticity thickness are larger than
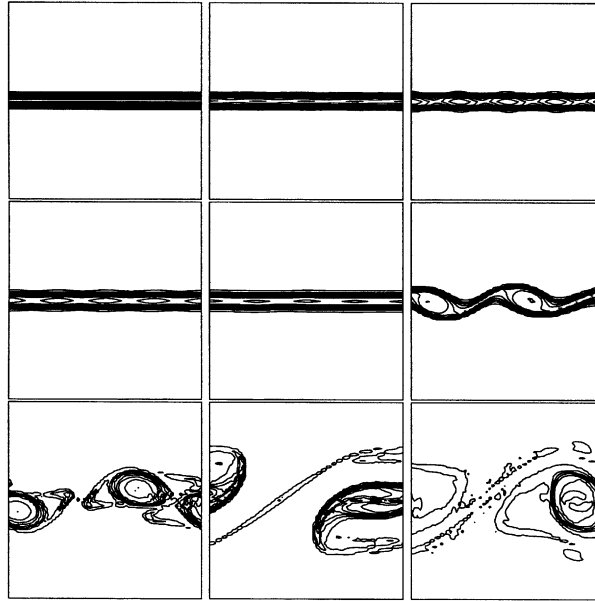
Fig. 5. Rational LES model with Smagorinsky model (12) as subgrid scale model and $c_S = 0.01$, vorticity on level 5, at time units 20, 30, 50, 70, 80, 100, 120, 140, 200 (left to right, top to bottom).

the values of the reference solution which indicates that the final eddy computed with the LES model is larger. The position of the final eddy is computed well.

4.2.2. The scaling factor $c_S = 0.005$

The results computed with the scaling factor $c_S = 0.005$ are presented in Fig. 6. It can be observed that there are great differences to the results obtained with $c_S = 0.01$. In the comparison of these results, it will be mentioned only if one result is better or worse than the other one. If there is no statement of comparison, the results are considered to be similar good or bad.

- *Development of the four primary eddies.* The four primary eddies can be seen clearly at time unit 30. They are present already at time unit 20. The rapid increase of the relative vorticity thickness from 1 to 2 can be seen in Fig. 10. The pairing starts a bit too early. This phase of the flow is computed much better than with the scaling factor $c_S = 0.01$.
- *Pairing of the four primary eddies.* The pairing of the four primary eddies is computed completely wrong, see Fig. 6. The four primary eddies are disappeared in time units 70 and 80 and a rather strange flow pattern can be seen. The secondary eddies in time unit 100 look rather the same. Thus, a nonsimultaneous pairing did not happen.
- *Pairing of the two secondary eddies.* The two secondary eddies are present at time unit 100. Then, there is some delay before their pairing starts. It starts at around time unit 150. Since there was no delay between both pairings, like in the reference solution, this phase of the flow was predicted better for the scaling factor $c_S = 0.01$.
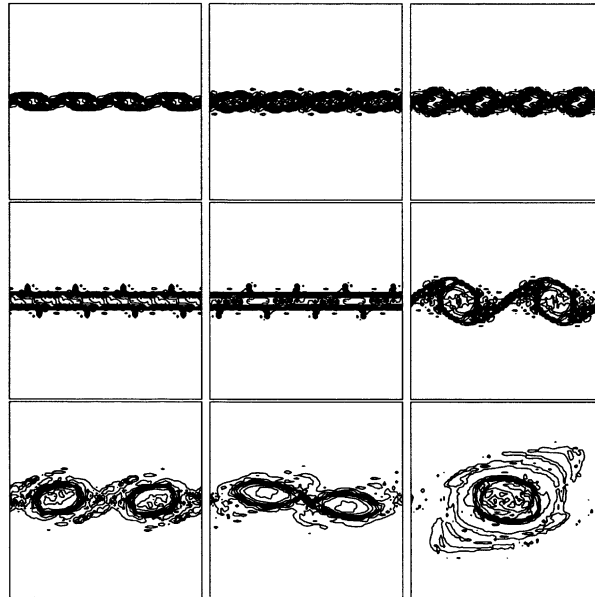
Fig. 6. Rational LES model with Smagorinsky model (12) as subgrid scale model and $c_S = 0.005$, vorticity on level 5, at time units 20, 30, 50, 70, 80, 100, 120, 140, 200 (left to right, top to bottom).

- *Rotation of the final eddy.* The rotation of the final eddy happens with a speed which is too small and a relative vorticity thickness which is too large. But, compared to the results obtained with $c_S = 0.01$, the values and the frequency of the relative vorticity thickness are closer to the reference solution. The position of the final eddy is wrong.

The solution is much more noisy for $c_S = 0.005$. The total kinetic energy of the velocity, Fig. 11, is predicted somewhat better for $c_S = 0.005$.

Considering the whole time interval, the results for $c_S = 0.01$ are better. The results for $c_S = 0.005$ are completely wrong after the first phase of the flow.

4.3. The rational LES model with Iliescu–Layton subgrid scale term

The rational LES model with Iliescu–Layton subgrid scale term (14) was applied with the scaling factors $c_S = 0.5$ and 0.17. The use of the scaling factor $c_S = 0.17$ is proposed in [20].

4.3.1. The scaling factor $c_S = 0.5$
The development of the vorticity using $c_S = 0.5$ is presented in Fig. 7.

- *Development of the four primary eddies.* The primary eddies are clearly visible already at time unit 20. This is somewhat too early. The development starts at around time unit 15 and a rather steep increase of the relative vorticity thickness from 1 to 2 can be observed, Fig. 10. A similar steep increase can be seen also for the reference solution.
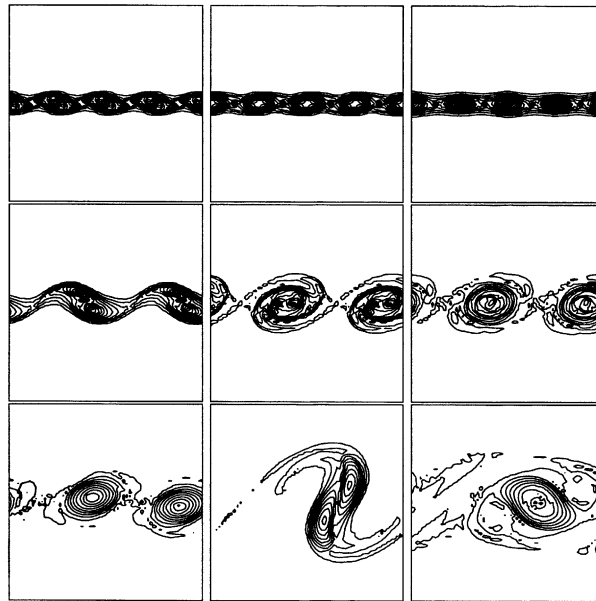
Fig. 7. Rational LES model with Iliescu–Layton model (14) as subgrid scale model and $c_S = 0.5$, vorticity on level 5, at time units 20, 30, 50, 70, 80, 100, 120, 140, 200 (left to right, top to bottom).

- *Pairing of the four primary eddies.* This pairing happens somewhat too early, at time unit 65. The sharp peak in the relative vorticity thickness can be seen very well. A non-simultaneous pairing of the four primary eddies cannot be observed.
- *Pairing of the two secondary eddies.* This pairing occurs, in contrast to the reference solution, not directly after the pairing of the four primary eddies. There is some delay and the pairing of the secondary eddies takes place too late, at around time unit 140.
- *Rotation of the final eddy.* The speed of the rotation of the final eddy is too small which is reflected in a too small frequency of the oscillation of the relative vorticity thickness. The values of the relative vorticity thickness are too large, which means that the final eddy is larger than in the reference solution.

4.3.2. The scaling factor $c_S = 0.17$

The development of the vorticity for the computations with the scaling factor $c_S = 0.17$ is presented in Fig. 8.

The computed results obtained with $c_S = 0.5$ and 0.17 are also compared here. It will be mentioned only if one result is considered better than the other one. If there is no statement of comparison, the results are considered to have a similar quality.

The computational results obtained with $c_S = 0.17$ are as follows:

- *Development of the four primary eddies.* The four primary eddies can be clearly seen at time unit 30. This development starts earlier than in the reference solution and the relative vorticity
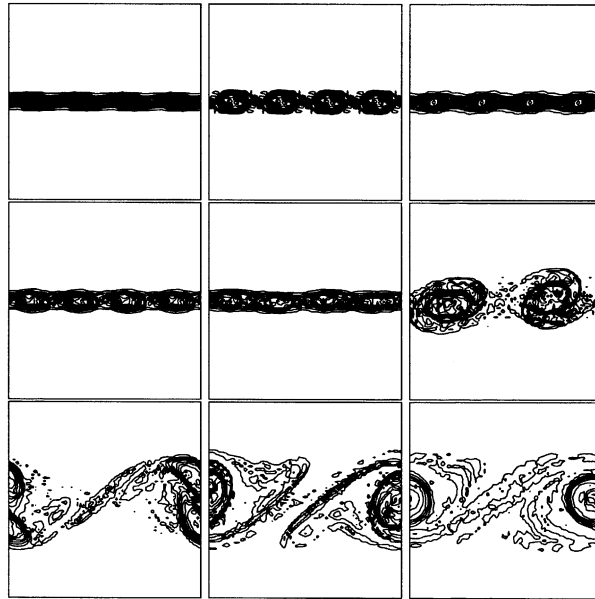
Fig. 8. Rational LES model with Iliescu–Layton model (14) as subgrid scale model and $c_S = 0.17$, vorticity on level 5, at time units 20, 30, 50, 70, 80, 100, 120, 140, 200 (left to right, top to bottom).
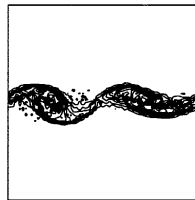

Fig. 9. Rational LES model and Iliescu–Layton model (14) as subgrid scale model with $c_S = 0.17$, time unit 90.

thickness increases moderately, see Fig. 10. The increase of the relative vorticity thickness is computed a little bit better with the scaling factor $c_S = 0.5$.

- *Pairing of the four primary eddies.* This pairing starts somewhat too late, after time unit 80. But for this LES model, one can observe the nonsimultaneous pairing of the four primary eddies, see especially time unit 90 in Fig. 9. This pairing is computed much better than with all other considered LES models.
- *Pairing of the two secondary eddies.* This LES model behaves further similar to the reference solution. Immediately after the pairing of the four primary eddies starts the pairing of the two secondary eddies. Since the former pairing occurred too late, also the pairing of the secondary eddies happens somewhat too late, at around time unit 120. This phase of the flow is computed better with $c_S = 0.17$.
- *Rotation of the final eddy.* Like in all other computations on level 5, the speed of the rotation of the final eddy and the frequency of the oscillation of the relative vorticity thickness are too small. The position of the final eddy is computed well.
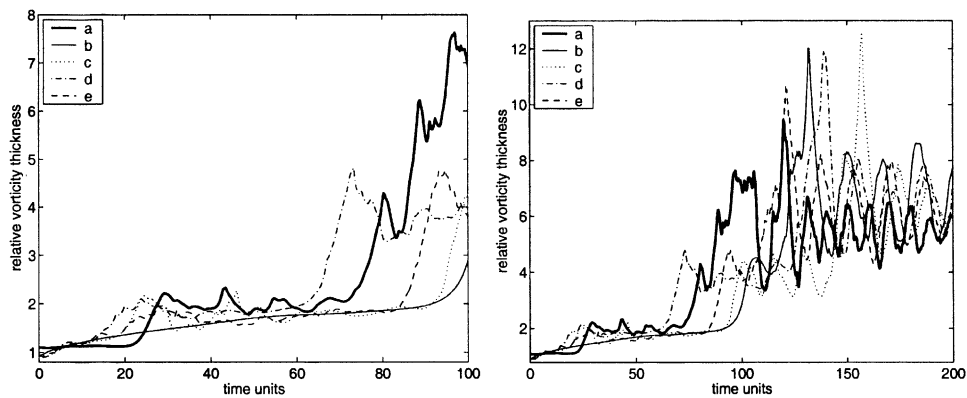
Fig. 10. Relative vorticity thickness to σ_0, level 5; a—convolution of DNS solution, b—rational LES model with Smagorinsky subgrid scale model ($c_S = 0.01$), c—rational LES model with Smagorinsky subgrid scale model ($c_S = 0.005$), d—rational LES model with Iliescu–Layton subgrid scale model ($c_S = 0.5$), e—rational LES model with Iliescu–Layton subgrid scale model ($c_S = 0.17$).

The total kinetic energy of the velocity, Fig. 11, is predicted more accurately with $c_S = 0.17$. Altogether, the rational LES model with Iliescu–Layton subgrid scale model and $c_S = 0.17$ was in nearly all considered aspects superior to the simulations with $c_S = 0.5$. Especially, the computation of the nonsimultaneous pairing of the four primary eddies is remarkable.

4.4. A comparison of the results obtained with the Smagorinsky subgrid scale model and the Iliescu–Layton subgrid scale model

In this section, both models of the subgrid scale term are compared, based on the best solution in each case. The evaluation of the numerical studies with the Smagorinsky subgrid scale model came to the conclusion that the result obtained with $c_S = 0.01$ is better. Using the Iliescu–Layton subgrid scale model, the rational LES model with $c_S = 0.17$ performed best.

- The results obtained with the Iliescu–Layton subgrid scale term are better in the following respects:
  - The computation of the four primary eddies is better. They are not as flat as computed with the Smagorinsky subgrid scale model.
  - The pairing of the four primary eddies is computed much better. Especially that a nonsimultaneous pairing is observed, like in the reference solution, is very remarkable.
  - The times of the pairings are closer to the reference solution.
- The results obtained with the Smagorinsky subgrid scale term are better in the following respects:
  - The total kinetic energy of the velocity is predicted somewhat more accurately.
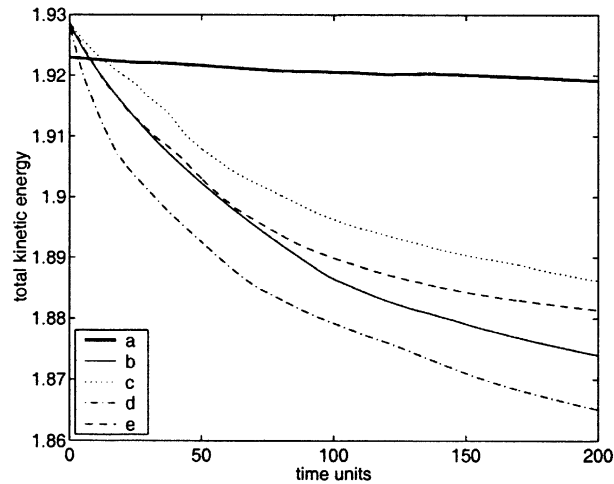 - The position of the final eddy is computed a little bit better.

Fig. 11. Total kinetic energy of the velocity, level 5; a—convolution of DNS solution, b—rational LES model with Smagorinsky subgrid scale model ($c_S = 0.01$), c—rational LES model with Smagorinsky subgrid scale model ($c_S = 0.005$), d—rational LES model with Iliescu–Layton subgrid scale model ($c_S = 0.5$), e—rational LES model with Iliescu–Layton subgrid scale model ($c_S = 0.17$).

- The following features of the reference solution are reproduced insufficiently by the solutions obtained with both variants of the subgrid scale term:
  ○ In general, the pairings of the eddies occur at somewhat different times as in the reference solution.
  ○ The speed of rotation of the final eddy is too small.

In summary, the rational LES model with Iliescu–Layton subgrid scale term and $c_S = 0.17$ computed the main features of the flow better in our numerical study.

In addition, the quality of the results obtained with the Iliescu–Layton subgrid scale model and $c_S = 0.5$ is comparable with the Smagorinsky subgrid scale model and $c_S = 0.01$. Both results have the same shortcomings, in particular, a simultaneous pairing of the four primary eddies. In contrast, the result computed with the Smagorinsky subgrid scale model and $c_S = 0.005$ is much worse than both results obtained with the Iliescu–Layton subgrid scale model, above all in the initial phase of the flow. Altogether, considering all results, the prediction of the space averaged flow was better with the Iliescu–Layton subgrid scale model.

5. A mixing layer problem in three dimensions

The mixing layer problem is also an often used test problem for turbulent flow simulations in three dimensions. Computations with this problem can be found, e.g. in [4,9,27,31].

5.1. The definition of the problem and the set-up of the numerical tests

5.1.1. The definition of the problem

We define this problem similarly to the 2d mixing layer problem. The domain of computation is $\Omega = (-1, 1) \times (-2, 2) \times (0, 2)$. It was important to extend the computational domain in y direction compared to the 2d mixing layer problem in order that the eddies can develop undisturbed by the y boundary. Free-slip boundary conditions are applied at $y = -2$ and 2. On the other four boundaries, periodic boundary conditions are prescribed. The initial velocity is given by

$$
\mathbf{w}_0 = \begin{pmatrix} W_\infty \tanh\left(\dfrac{2y}{\sigma_0}\right) \\ 0 \\ 0 \end{pmatrix} + c_{\text{noise}} W_\infty \begin{pmatrix} \dfrac{\partial \psi}{\partial y} + \dfrac{\partial \psi}{\partial z} \\ -\dfrac{\partial \psi}{\partial x} \\ -\dfrac{\partial \psi}{\partial x} \end{pmatrix} \tag{20}
$$

with

$$
\psi = \exp(-(2y/\sigma_0)^2)(\cos(\pi x) + \cos(2\pi z)).
$$

The parameters are chosen in the computations as follows: $W_\infty = 1$, scaling factor $c_{\text{noise}} = 0.01$ and the initial vorticity thickness $\sigma_0 = 1/14$. The Reynolds number is defined by $Re = \sigma_0 W_\infty / \nu$. We will present computations for $\nu = 1/2800$, i.e. $Re = 200$. This Reynolds number is somewhat larger than the Reynolds numbers which are used in [4,9,31]. For $Re = 200$, the solution of the Navier–Stokes equations with Galerkin finite element discretisation (DNS) was possible on refinement level 4 of the initial grid, see Table 2 for information on the grids. Already for $Re = 250$, the DNS blew up. The DNS solution is filtered and then used as reference solution for the LES models in the same fashion as it was done in the 2d mixing layer problem, Section 4.

5.1.2. The momentum thickness

In the 3d mixing layer problem, it is common to use the momentum thickness instead of the vorticity thickness for evaluating the numerical simulations [27,31]. Let $\Omega = (x_0, x_1) \times (-y_0, y_0) \times (z_0, z_1)$ with $y_0 > 0$. The momentum thickness $\mu(t)$ is given by

$$
\mu(t) = \int_{-y_0}^{y_0} \left(\frac{1}{4} - \left(\frac{\langle w_1 \rangle(t, y)}{2W_\infty} \right)^2 \right) \, dy,
$$

Table 2
Degrees of freedom and mesh width on different levels

Level	h	Velocity	Pressure	Total
0	$\sqrt{3}$	432	64	494
3	$\sqrt{3}/8$	199 680	32 768	232 448
4	$\sqrt{3}/16$	1 585 152	262 144	1 847 296

where w_1 is the first component of the velocity and

$$\langle w_1 \rangle (t, y) = \frac{\int_{x_0}^{x_1} \int_{z_0}^{z_1} w_1(t, x, y, z) \, dz \, dx}{\int_{x_0}^{x_1} \int_{z_0}^{z_1} \, dz \, dx}.$$

For the undisturbed initial velocity, $c_{\text{noise}} = 0$, a straightforward computation gives $\mu(0) \approx \sigma_0/4$. We set $\mu_0 = 1/56$ and present in the evaluation of the numerical results the relative momentum thickness $\mu(t)/\mu_0$. The momentum thickness is an integral quantity while the vorticity thickness is obtained by differentiation. Thus, the momentum thickness will be smoother and less sensitive to noise in the flow.

5.1.3. The discretisation in time and space, parameters of the LES models

The numerical studies presented in this section were performed with the fractional-step θ-scheme as discretisation in time and the Q_2/P_1^{disc} finite element spatial discretisation. A time unit $\bar{t}$ is defined by $\bar{t} = \sigma_0/W_\infty$. The time discretisation was applied with an equal distant time step of $\Delta t_n = 0.5\bar{t} = 1/28 \approx 3.5714e - 2$ and the final time was set to be $T = 40\bar{t} \approx 2.8507$. The initial grid (level 0) consists of 16 cubes of edge length one. This grid is refined uniformly. The computations with the rational LES model are carried out on level 3. The number of the degrees of freedom and the mesh width are given in Table 2. The filter width $\delta = h$ was used in all tests.

The auxiliary problems which have to be solved in the rational LES model and in the Iliescu–Layton subgrid scale model are equipped with periodic boundary conditions on all boundaries on which the mixing layer problem possesses such boundary conditions. On the other two boundaries, homogeneous Neumann boundary conditions are prescribed.

5.2. The evaluation of the numerical results

The evaluation of the numerical results is based on:

- the z-component of the vorticity in the plane $z = 1$, where the part $(-1, 1) \times (-1, 1)$ of the cut plane is presented. The isolines are drawn at the values $\pm k + 0.5, k = 0, 1, \ldots,$
- the relative momentum thickness $\mu(t)/\mu_0$,
- the total kinetic energy.

The reference solution is presented in Fig. 12. At time unit 10, four large eddies are present. The interior of these eddies is already rather unstructured. Between time unit 10 and 20, a pairing occurs such that at time unit 20 two large flow structures are visible. Two flow structures can be observed still at time unit 40. After this time, the flow becomes completely unstructured. The relative momentum thickness of the filtered discrete velocity, Fig. 15, is monotonically increasing. The steep increase at the beginning corresponds to the formation of the first eddies from the initial noise. The total kinetic energy is monotonically decreasing, Fig. 16.

The grid which was used for the LES simulations is too coarse to admit a DNS and to apply the rational LES model without model for the subgrid scale term. Both simulations blew up later than at time unit 40 but the computed results were completely wrong already at time unit 20. Thus, the use of a model for the subgrid scale term becomes necessary. Since the Reynolds number of the
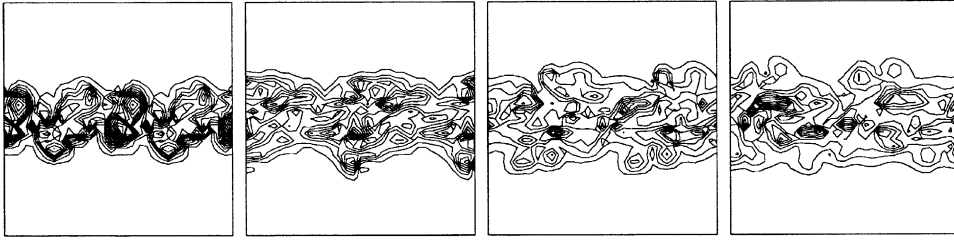
Fig. 12. 3d mixing layer problem, $Re = 200$, vorticity of $\overline{\mathbf{u}^h}$, level 4, at time units 10, 20, 30, 40.
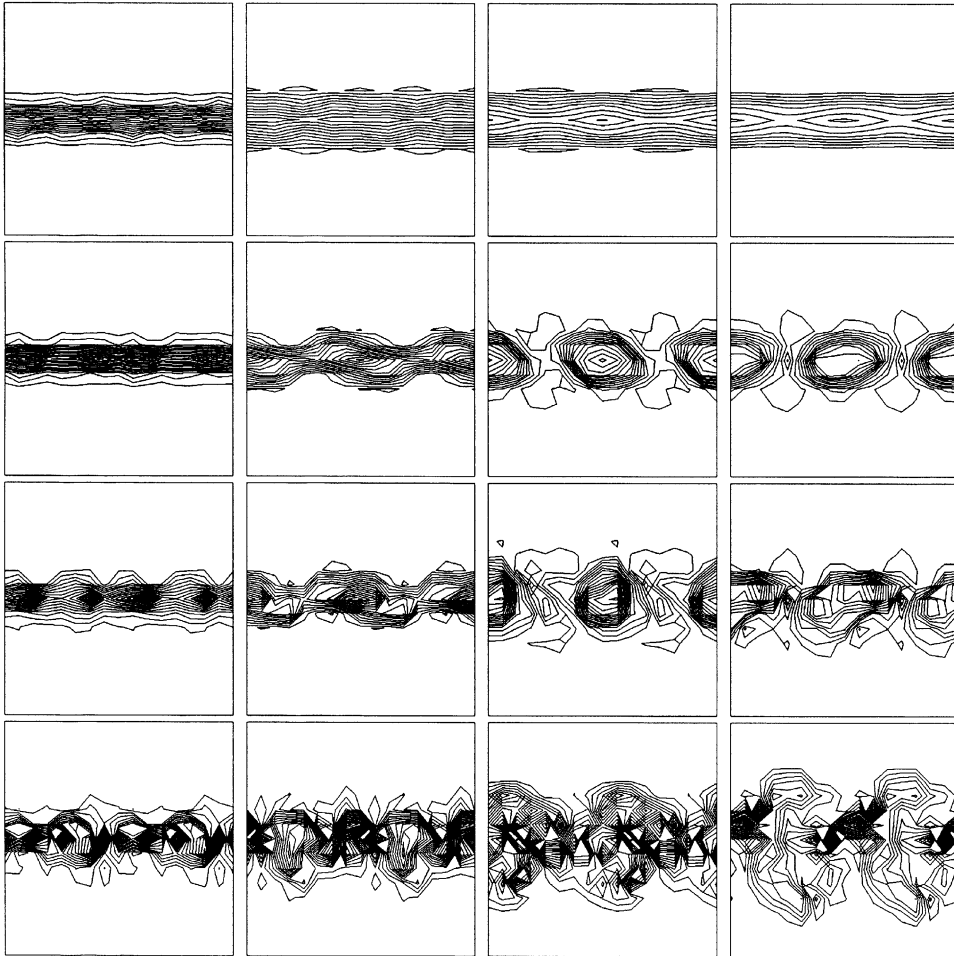

Fig. 13. 3d mixing layer problem, $Re = 200$, rational LES model with Smagorinsky model (12) as subgrid scale model and $c_S = 0.01, 0.005, 0.0025, 0.001$ (top to bottom), vorticity on level 3, at time units 10, 20, 30, 40 (left to right).

flow in this example is small compared to realistic turbulent flows, it is not clear if the values for c_S used for realistic flows should be applied in this example or smaller ones. For this reason, the behaviour of the models is studied for both cases.
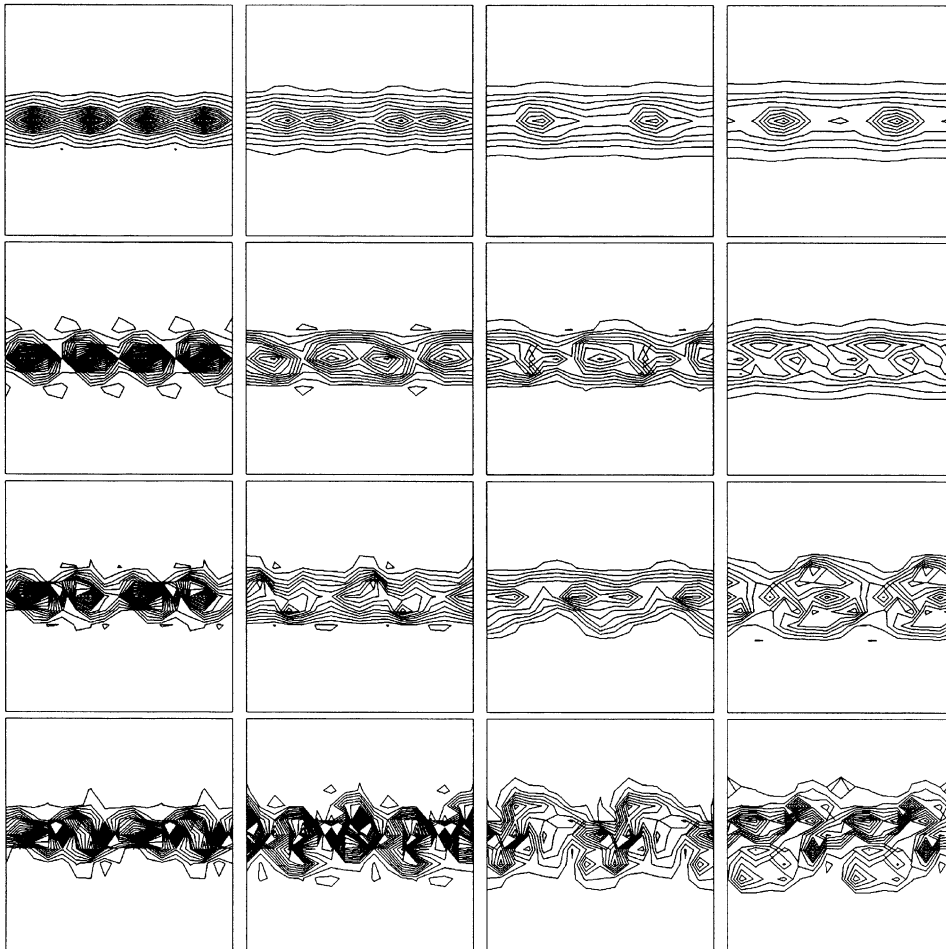
Fig. 14. 3d mixing layer problem, $Re = 200$, rational LES model with Iliescu–Layton model (14) as subgrid scale model and $c_S = 0.5, 0.1, 0.05, 0.025$ (top to bottom), vorticity on level 3, at time units 10, 20, 30, 40 (left to right).

The evolution of the flow for the rational LES model with Smagorinsky subgrid scale term and different values of c_S is presented in Fig. 13. For the values $c_S = 0.01$ and 0.005, the solutions are much smoother than the reference solution. The pairing from two to four eddies occurred for all values of c_S between time unit 10 and 20. In all cases, these two flow structures stay until time unit 40 and they posses more internal structure than in the reference solution. The best results with respect to the relative momentum thickness and the total kinetic energy were obtained with $c_S = 0.001$.

The computational results for the Iliescu–Layton subgrid scale model are presented in Fig. 14. For the large values $c_S = 0.5$ and 0.1, the solutions are too smooth. The pairing from two to four flow structures occurred for all values of c_S later than in the reference solution, between time unit 20 and 30. The two eddies at the final time unit 40 are in all cases more structured than in the
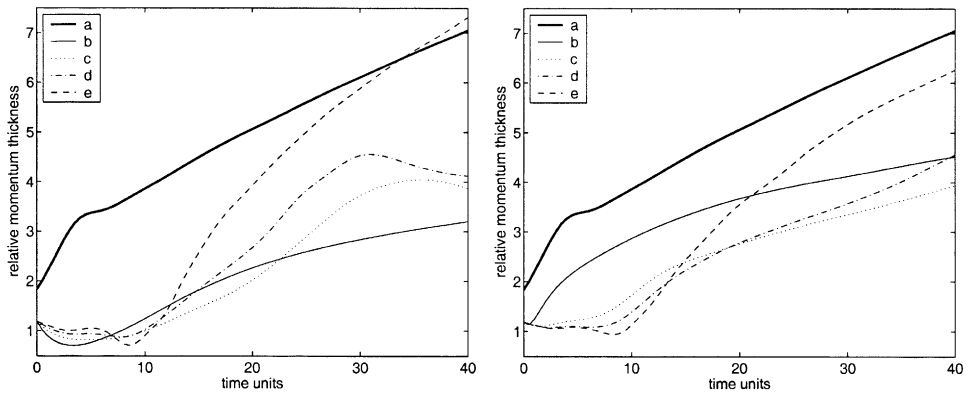
Fig. 15. 3d mixing layer problem, $Re = 200$, relative momentum thickness, a: filtered DNS solution, left: rational LES model with Smagorinsky subgrid scale model (b: $c_S = 0.01$, c: $c_S = 0.005$ d: $c_S = 0.0025$, e: $c_S = 0.001$), right: rational LES model with Iliescu–Layton subgrid scale model b: $c_S = 0.5$, c: $c_S = 0.1$ d: $c_S = 0.05$, e: $c_S = 0.025$).
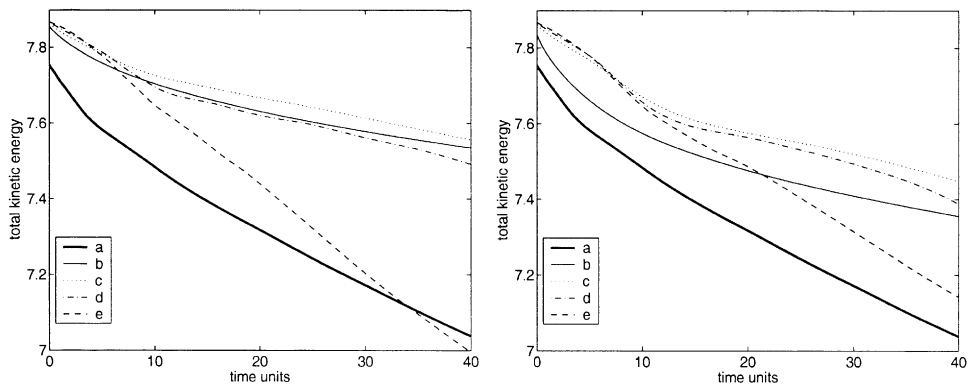

Fig. 16. 3d mixing layer problem, $Re = 200$, total kinetic energy, a: filtered DNS solution, left: rational LES model with Smagorinsky subgrid scale model (b: $c_S = 0.01$, c: $c_S = 0.005$ d: $c_S = 0.0025$, e: $c_S = 0.001$), right: rational LES model with Iliescu–Layton subgrid scale model b: $c_S = 0.5$, c: $c_S = 0.1$ d: $c_S = 0.05$, e: $c_S = 0.025$).

reference solution. With respect to the relative momentum thickness and the total kinetic energy, the best results were obtained with $c_S = 0.025$.

In summary, there are no distinct differences between the results obtained with both models for the subgrid scale term in the 3d mixing layer problem. For large values of c_S, the computed solutions were too smooth, especially for the Smagorinsky model. Also for small c_S, the computed flows posses more structure than in the reference solution. The time of the pairing of the four initial eddies was predicted somewhat better using the Smagorinsky subgrid scale model.

6. Summary

This paper compared two models for the subgrid scale tensor used within the rational LES model: the Smagorinsky subgrid scale model and the Iliescu–Layton subgrid scale model. The solutions obtained with these models were compared to filtered DNS data in a 2d mixing layer problem at $Re = 10\,000$ and a 3d mixing layer problem at $Re = 200$. Whereas the Iliescu–Layton subgrid scale model proved to be better in the 2d study, the results obtained with both models in the 3d study were similar. However, the computed solutions with both models for the subgrid scale term showed also a number of shortcomings.

One negative aspect is that the results depend on the scaling factor c_S. For the Smagorinsky LES model, a dynamical procedure has been developed for computing c_S a posteriori as a function in time and space [8,24]. This approach has to be extended yet to the rational LES model. Its development will certainly improve the model and reduce its shortcomings. This will be future work.

References

[1] B.J. Boersma, M.N. Kooper, F.T.M. Neuwstadt, P. Wesseling, Local grid refinement in large-eddy simulations, J. Enrg. Math. 32 (1997) 161–175.

[2] R.A. Clark, J.H. Ferziger, W.C. Reynolds, Evaluation of subgrid-scale models using an accurately simulated turbulent flow, J. Fluid Mech. 91 (1979) 1–16.

[3] P. Coletti, Analytic and numerical results for $k - \varepsilon$ and large eddy simulation turbulence models, Ph.D. Thesis, University of Trento, 1998.

[4] P. Comte, M. Lesieur, E. Lamballais, Large- and small-scale stirring of vorticity and a passive scalar in a 3-d temporal mixing layer, Phys. Fluids A 4 (12) (1992) 2761–2778.

[5] A. Dunca, V. John, W.J. Layton, The commutation error of the space averaged Navier–Stokes equations on a bounded domain, J. Math. Fluid Mech. (2004), accepted for publication.

[6] M. Fortin, Finite element solution of the Navier–Stokes equations, in: A. Iserles (Ed.), Acta Numerica, Cambridge University Press, Cambridge, 1993, pp. 239–284.

[7] G.P. Galdi, W.J. Layton, Approximation of the larger eddies in fluid motion II: a model for space filtered flow, Math. Model Methods Appl. Sci. 10 (3) (2000) 343–350.

[8] M. Germano, U. Piomelli, P. Moin, W. Cabot, A dynamic subgrid-scale eddy viscosity model, Phys. Fluids A 3 (1991) 1760–1765.

[9] B.J. Geurts, D.D. Holm. Leray simulation of turbulent shear layers. in I.P. Castro, P.E. Hancock, T.G. Thomas (Eds.), Advances in Turbulence IX, CIMNE, Barcelona, 2002, pp. 337–340.

[10] P.M. Gresho, R.L. Sani, Incompressible Flow and the Finite Element Method, Wiley, Chichester, 2000.

[11] M. Griebel, F. Koster, Adaptive wavelet solvers for the unsteady incompressible Navier–Stokes equations, in: J. Malek, J. Nečas, M. Rokyta (Eds.), Advances in Mathematical Fluid Mechanics, Springer, Berlin, 2000, pp. 67–118.

[12] T. Iliescu, V. John, W.J. Layton, G. Matthies, L. Tobiska, A numerical study of a class of LES models, Internat. J. Comput. Fluid Dynamics 17 (2003) 75–85.

[13] T. Iliescu, W.J. Layton, Approximating the larger eddies in fluid motion III: the Boussinesq model for turbulent fluctuations, An. Ştiinţ. Univ. "Al. I. Cuza" Iaşi Tomul XLIV Sect. I.a Mat. 44 (1998) 245–261.

[14] V. John, Higher order finite element methods and multigrid solvers in a benchmark problem for the 3D Navier–Stokes equations, Internat. J. Numer. Methods Fluids 40 (2002) 775–798.

[15] V. John, Large Eddy Simulation of Turbulent Incompressible Flows, Analytical and Numerical Results for a Class of LES Models, Vol. 34, Lecture Notes in Computational Science and Engineering, Springer, Berlin, Heidelberg, New York, 2003.

[16] V. John, W.J. Layton, Analysis of numerical errors in large eddy simulation, SIAM J. Numer. Anal. 40 (2002) 995–1020.

[17] V. John, G. Matthies, Higher order finite element discretizations in a benchmark problem for incompressible flows, Internat. J. Numer. Methods Fluids 37 (2001) 885–903.

[18] V. John, G. Matthies, MooNMD—a program package based on mapped finite element methods, Comput. Visual. Sci. 6 (2004) 163–170.

[19] O.A. Ladyzhenskaya, New equations for the description of motion of viscous incompressible fluids and solvability in the large of boundary value problems for them, Proc. Steklov Inst. Math. 102 (1967) 95–118.

[20] W.J. Layton, R. Lewandowski, Analysis of an eddy viscosity model for large eddy simulation of turbulent flows, J. Math. Fluid Mech. 4 (2002) 374–399.

[21] A. Leonard, Energy cascade in large eddy simulation of turbulent fluid flows, Adv. Geophys. 18A (1974) 237–248.

[22] M. Lesieur, Turbulence in Fluids, Fluid Mechanics and its Applications, Vol. 40, 3rd Edition, Kluwer Academic Publishers, Dordrecht, 1997.

[23] M. Lesieur, C. Staquet, P. Le Roy, P. Comte, The mixing layer and its coherence examined from the point of view of two-dimensional turbulence, J. Fluid Mech. 192 (1988) 511–534.

[24] D.K. Lilly, A proposed modification of the Germano subgrid-scale closure method, Phys. Fluids A 4 (1992) 633–635.

[25] A. Michalke, On the inviscid instability of the hyperbolic tangent velocity profile, J. Fluid Mech. 19 (1964) 543–556.

[26] S. Nägele, G. Wittum, Large-eddy simulation and multigrid methods, Electon. Trans. Numer. Anal. 15 (2003) 152–164.

[27] M.M. Rogers, R.D. Moser, Direct simulation of a self-similar turbulent flow, Phys. Fluids 6 (1994) 903–923.

[28] P. Sagaut, Large Eddy Simulation for Incompressible Flows, Springer, Berlin, Heidelberg, New York, 2001.

[29] J.S. Smagorinsky, General circulation experiments with the primitive equations, Monthly Weather Rev. 91 (1963) 99–164.

[30] S. Turek, Efficient Solvers for Incompressible Flow Problems: an Algorithmic and Computational Approach, in: Lecture Notes in Computational Science and Engineering, Vol. 6, Springer, Berlin, 1999.

[31] B. Vreman, B. Guerts, H. Kuerten, Large-eddy simulation of turbulent mixing layer, J. Fluid Mech. 339 (1997) 357–390.

[32] Y. Zang, R.L. Street, J.R. Koseff, A dynamic mixed subgrid-scale model and its application to turbulent recirculating flows, Phys. Fluids A 5 (1993) 3186–3196.